ce/papers
The online collection for conference papers in civil engineering
Ernst & Sohn A Wiley Brand

ORIGINAL ARTICLE

eurosteel SHEFFIELD 2021
Ernst & Sohn A Wiley Brand

A Numerical Approach for Plastic Cross-Sectional Analyses of Steel Members

Stalin Ibáñez[1], Matthias Kraus[1]

Correspondence

Prof. Dr. Matthias Kraus
Bauhaus University of Weimar
Chair of Steel and Hybrid Structures
Marienstraße 13D
99423 Weimar, Germany
Email: matthias.kraus@uni-weimar.de

Affiliations

[1]Bauhaus University of Weimar, Chair of Steel and Hybrid Structures, Weimar, Germany

Abstract

Global structural analyses in civil engineering are usually performed considering linear-elastic material behavior. However, for steel structures, a certain degree of plasticization depending on the member classification may be considered. Corresponding plastic analyses taking material nonlinearities into account are effectively realized using numerical methods. Frequently applied finite elements of two and three-dimensional models evaluate the plasticity at defined nodes using a yield surface, i.e. by a yield condition, hardening rule, and flow rule. Corresponding calculations are connected to a large numerical as well as time-consuming effort and they do not rely on the theoretical background of beam theory, to which the regulations of standards mainly correspond. For that reason, methods using beam elements (one-dimensional) combined with cross-sectional analyses are commonly applied for steel members in terms of plastic zones theories. In these approaches, plasticization is in general assessed by means of axial stress only. In this paper, more precise numerical representation of the combined stress states, i.e. axial and shear stresses, is presented and results of the proposed approach are validated and discussed.

Keywords

Plasticity, plastic analysis, plastic zones theory, cross-section, beam theory

1 Introduction

The design of steel structures and members can be performed based on plastic structural analyses. Corresponding investigations usually rely on beam theory, i.e. finite element methods (FEM) based on one-dimensional elements, due to the specifications in codes as well as advantages for interpretations. However, for plastic structural analyses incorporating plastic internal forces and capacities, advanced procedures are necessary.

General formulations regarding material plasticity have been presented in literature by many authors, see for example [1]-[4]. The formulations are universally developed for any possible stress state. Moreover, for evaluating the plastic states of structures using FEM, incremental and iterative analyses are in general necessary, i.e. loads need to be applied in small steps to follow the yielding process by iterative procedures. For obtaining the proper stress development, fine element meshes are necessary. Consequently, analyses of structures considering plasticity require high computational demands. In literature, efforts are carried out for improvements in this context. For example, Krabbenhoft [5] presents the theory of plasticity for membrane elements, considering axial stresses and shear stresses components. While in [6], Öchsner shows the evaluation of plasticity in frame structures, comparing analytical solutions with computational implementations as well as introducing specific solutions for beam elements. In [7], Kindmann and Kraus have presented an approach that combines cross-section elements with beam elements for analysing plasticity in structures. Figure 1 shows an example of the geometrically and physically nonlinear structural analysis with imperfections of a crane runway girder based on the procedure. The method considers axial stress with reductions due to shear by approximation. Chen and Trahair introduce a similar approach in [8] combining cross-section and beam elements for analysing torsional effects in beams.

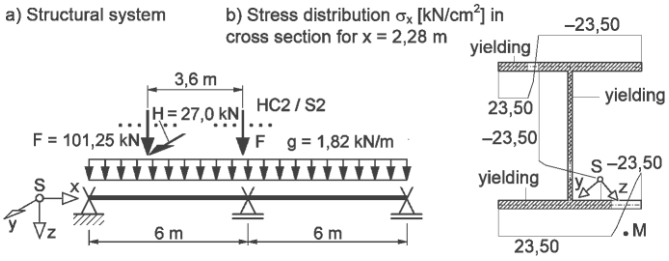

Figure 1 Plastic structural analysis of a crane runway girder according to [7]

In this paper, a simplified procedure for evaluating cross-section

plasticization for thin walled cross-sections is introduced, by combining a middle line cross-section model with plastic analyses regarding axial and shear stresses. For this purpose, fundamental mechanical formulations of plasticity theory (yield condition, hardening rule, and flow rule) appropriate for steel are introduced and adjusted to the stress field of beam cross-sections. With respect to thin walled cross-sections, algorithms for numerical implementations and calculation results are exemplified as well as discussed.

2 Plasticity

2.1 Fundamental relationships

Figure 2a shows the behaviour of steel in terms of a technical stress-strain-diagram determined by a tensile test with a fundamental distinction of an elastic and plastic material behaviour. It is common practice to idealize the constitutive relationship using a bilinear approach as shown in Figure 2b, in which the slope of the elastic region is defined by the modulus of elasticity E and the one in the plastic range using a tangent modulus E_v. The relations in Figure 2b are not drawn to scale regarding structural steel for reasons of better exemplifications.

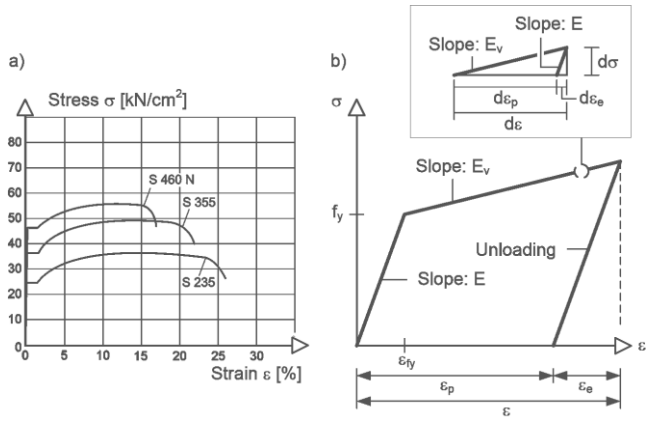

Figure 2 Stress-strain relationship of steel

According to Figure 2b strain ε can be subdivided into an elastic ε_e and a plastic component ε_p:

$$\varepsilon = \varepsilon_e + \varepsilon_p \tag{1}$$

Using Hooke's law, stress is connected to corresponding elastic strain as follows:

$$\sigma = E \cdot \varepsilon_e = E \cdot (\varepsilon - \varepsilon_p) \tag{2}$$

On the other hand, it is possible to describe the incremental change of stress in the plastic zone in dependency of a strain increment. According to [9], the following relationship is obtained (see Figure 2b):

$$d\sigma = H \cdot d\varepsilon_p \quad \text{with} \quad H = \frac{E \cdot E_v}{E - E_v} \tag{3}$$

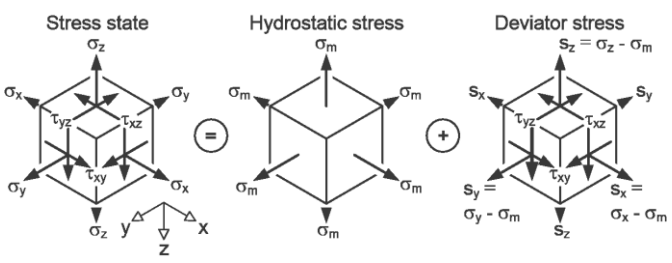

Figure 3 Spatial stress state

Transferring to a spatial stress state described by stress $\underline{\boldsymbol{\sigma}}$ (Figure 3) and strain tensors $\underline{\boldsymbol{\varepsilon}}$ (indicated using underlined and bold letters), Equation (2) yields to:

$$\underline{\boldsymbol{\sigma}} = \underline{\boldsymbol{C}}_e : (\underline{\boldsymbol{\varepsilon}} - \underline{\boldsymbol{\varepsilon}}_p) \tag{4}$$

$$\text{with} \quad \underline{\boldsymbol{\sigma}} = \begin{bmatrix} \sigma_x & \tau_{xy} & \tau_{xz} \\ \tau_{yx} & \sigma_y & \tau_{yz} \\ \tau_{zx} & \tau_{zy} & \sigma_z \end{bmatrix} \quad \text{and} \quad \underline{\boldsymbol{\varepsilon}} = \begin{bmatrix} \varepsilon_x & \varepsilon_{xy} & \varepsilon_{xz} \\ \varepsilon_{yx} & \varepsilon_y & \varepsilon_{yz} \\ \varepsilon_{zx} & \varepsilon_{zy} & \varepsilon_z \end{bmatrix}$$

Shear strains are connected to the relations $\gamma_{xy} = 2 \cdot \varepsilon_{xy}$, $\gamma_{yz} = 2 \cdot \varepsilon_{yz}$, and $\gamma_{xz} = 2 \cdot \varepsilon_{xy}$. In Equation (4), $\underline{\boldsymbol{C}}_e$ is the elasticity tensor. The stress tensor $\underline{\boldsymbol{\sigma}}$ can be subdivided into hydrostatic $\sigma_m \cdot \underline{\boldsymbol{\delta}}$ and deviator stresses $\underline{\boldsymbol{s}}$ as shown in Figure 3:

$$\underline{\boldsymbol{\sigma}} = \sigma_m \cdot \begin{bmatrix} 1 & 0 & 0 \\ 0 & 1 & 0 \\ 0 & 0 & 1 \end{bmatrix} + \begin{bmatrix} \sigma_x - \sigma_m & \tau_{xy} & \tau_{xz} \\ \tau_{yx} & \sigma_y - \sigma_m & \tau_{yz} \\ \tau_{zx} & \tau_{zy} & \sigma_{z-\sigma_m} \end{bmatrix} = \sigma_m \cdot \underline{\boldsymbol{\delta}} + \underline{\boldsymbol{s}} \tag{5}$$

$$\text{with} \quad \sigma_m = 1/3 \cdot (\sigma_x + \sigma_y + \sigma_z)$$

2.2 Yield condition

The yield condition F defines when steel begins to plasticise. Regarding the uniaxial stress state in Figure 2 and considering a linear elastic-ideal plastic material behaviour ($E_v = H = 0$), such a condition can be formulated using yield strength f_y :

$$F = \sigma_x - f_y = 0 \tag{6}$$

With $\sigma_x = f_y$, the condition for plasticising is fulfilled. To apply such a condition to a spatial stress state, an equivalent stress σ_V is being introduced:

$$F = \sigma_V^2 - f_y^2 = 0 \tag{7}$$

Squaring terms in Equation (7) is in general not necessary, however, helps to sometimes simplify formulations. The equivalent stress σ_V is derived using hypotheses of strength, where the energy of the acting spatial stress state is reduced to the single reference value σ_V (one-dimensional state). For steel the maximum distortion energy theorem shows good agreement to experiments. It presumes that the energy is characterised by distortions (without change of volume) connected to deviator stresses. With the derivations shown in [9], σ_V results in the following formula:

$$\sigma_V = \sqrt{\frac{3}{2} \underline{\boldsymbol{s}} : \underline{\boldsymbol{s}}} \tag{8}$$

Introducing the deviator stress tensor of Equation (5) gives the following equivalent stress:

$$\sigma_V = \sqrt{\sigma_x^2 + \sigma_y^2 + \sigma_z^2 - \sigma_x\sigma_y - \sigma_y\sigma_z - \sigma_x\sigma_z + 3\left(\tau_{xy}^2 + \tau_{yz}^2 + \tau_{xz}^2\right)} \tag{9}$$

Accounting for beam theory, in general only stresses σ_x, τ_{xy}, and τ_{xz} are existent going along with according simplifications. Introducing the equivalent stress into the yield condition (7) gives the formulation of Huber, v. Mises, Hencky, which is also referred to as v. Mises-criterion. It is the basis of the yield condition stated in Eurocode 3 [10]. Considering the space of principal stresses σ_1, σ_2 and σ_3, the criterion yields in a cylindrical yield surface shown in Figure 4, where elastic stress states ($F < 0$) are within the surface and plastic states ($F = 0$) on the surface.

2.3 Hardening rule – isotropic hardening

When a fibre of a steel member is stressed, it starts to plasticise when yield strength is reached and plastic strains ε_p occur, which remain in case the fibre is unloaded (see Figure 2). When restressing the fibre, yielding will now not be initiated at the stress level of yield strength, but at a higher stress – the steel shows strain hardening effects. This is covered in the yield condition (7) by adjusting the term of yield strength f_y:

$$F = \sigma_V^2 - \kappa^2\left(\varepsilon_{p,V}\right) = 0 \tag{10}$$

for $\varepsilon_{p,V} = 0$: $\kappa = f_y$ and $\varepsilon_{p,V} > 0$: $\kappa = f_y + H \cdot \varepsilon_{p,V}$

κ represents a strain hardening parameter depending on plastic strains. They are expressed by $\varepsilon_{p,V}$, i.e. an equivalent plastic strain, representing a reference value of a spatial strain state, comparable to σ_V. The influence of κ on the yield criterion is shown in Figure 4 with a widening of the yield surface. Since this affects all stress directions equally, it is referred to as isotropic hardening. Assuming an incompressibility of the material with constancy of volume, what can be appropriately adopted for steel, according to [9] an equivalent plastic strain increment can be determined as follows:

$$d\varepsilon_{p,V} = \sqrt{\frac{2}{3} d\underline{\boldsymbol{\varepsilon}}_{\boldsymbol{p}} : d\underline{\boldsymbol{\varepsilon}}_{\boldsymbol{p}}} \tag{11}$$

Increments $d\varepsilon_{p,V}$ will always be positive, having the effect, that the accumulated value $\varepsilon_{p,V}$ will continuously increase during load history going along with an enlargement of the limit function of the yield condition (10).

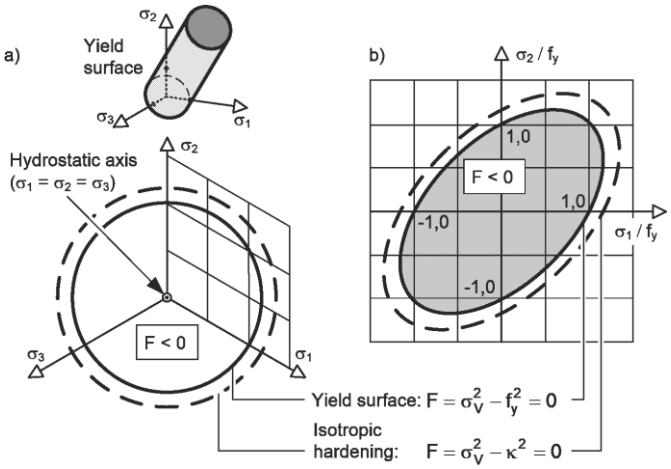

Figure 4 Yield surface of the v. Mises criterion and isotropic hardening in the space of principal stresses

2.4 Flow rule

The flow rule describes how the strain state changes during plasticization and in which direction plastic strains develop. Using the principle of the maximum plastic work, which goes back to v. Mises, the flow rule can be stated as follows [9]:

$$d\varepsilon_p = d\lambda \cdot \frac{\partial F}{\partial \underline{\sigma}} \tag{12}$$

With $\varepsilon_p^T = [\varepsilon_{p,x} \quad \varepsilon_{p,y} \quad \varepsilon_{p,z} \quad \gamma_{p,xy} \quad \gamma_{p,yz} \quad \gamma_{p,xz}]$

$$\left[\frac{\partial F}{\partial \underline{\sigma}}\right]^T = \left[\frac{\partial F}{\partial \sigma_x} \quad \frac{\partial F}{\partial \sigma_y} \quad \frac{\partial F}{\partial \sigma_z} \quad \frac{\partial F}{\partial \tau_{xy}} \quad \frac{\partial F}{\partial \tau_{yz}} \quad \frac{\partial F}{\partial \tau_{xz}}\right]$$

With regard to the formulations in the following section, a matrix formulation is used here. The derivatives of the yield condition describe the orientation of the strain increment, which is always perpendicular to the yield surface as shown in Figure 5 for the principal stress space. Since the flow rule is subjected to the yield condition, it is designated as so-called associated flow rule. $d\lambda$ is the proportionality factor or plastic multiplier, respectively, defining the size of the strain vector and therefore the quantity of plastic strains.

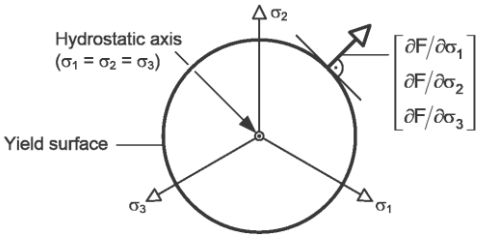

Figure 5 Orientation of the strain increment

According to [11], the flow rule can also be expressed for incompressible materials, which are described on the basis of the maximum distortion energy theorem, by:

$$d\underline{\boldsymbol{\varepsilon}}_{\boldsymbol{p}} = d\lambda \cdot 3 \cdot \underline{\boldsymbol{s}} \tag{13}$$

Using the expansion

$$d\underline{\boldsymbol{\varepsilon}}_{\boldsymbol{p}} : d\underline{\boldsymbol{\varepsilon}}_{\boldsymbol{p}} = d\lambda^2 \cdot 9 \cdot \underline{\boldsymbol{s}} : \underline{\boldsymbol{s}} \tag{14}$$

and introducing Equations (8) and (11) gives an expression for the plastic equivalent strain increment:

$$d\varepsilon_{p,V} = 2 \cdot d\lambda \cdot \sigma_V \tag{15}$$

With $F = 0$, the yield condition assures that stress states will always be on the yield surface in case of plasticising. However, this also has to be valid for variations of stress d$\underline{\sigma}$ and the yield start dκ, caused by changes of straining. For that reason, the variation of the yield condition dF has to satisfy the yield condition as well, i.e. $dF = 0$. This is formulated using the total differential of F:

$$\left[\frac{\partial F}{\partial \underline{\sigma}}\right]^T \cdot d\underline{\sigma} + \frac{\partial F}{\partial \kappa} \cdot d\kappa =$$

$$\left[\frac{\partial F}{\partial \underline{\sigma}}\right]^T \cdot \underline{C}_e \cdot d\underline{\varepsilon} - \left[\frac{\partial F}{\partial \underline{\sigma}}\right]^T \cdot \underline{C}_e \cdot d\underline{\varepsilon}_p - 2 \cdot \kappa \cdot H \cdot d\varepsilon_{p,V} = 0 \tag{16}$$

Condition (16) can be used to determine $d\lambda$. With the yield condition (10), when plasticising it is $\kappa = \sigma_V$. Considering this, the flow rule (12), and Equation (15) in Equation (16) gives the plastic multiplier $d\lambda$ to:

$$d\lambda = \frac{\left[\partial F/\partial \underline{\sigma}\right]^T \cdot \underline{C}_e \cdot d\underline{\varepsilon}}{\left[\partial F/\partial \underline{\sigma}\right]^T \cdot \underline{C}_e \cdot \partial F/\partial \underline{\sigma} + 4 \cdot H \cdot \sigma_V^2} \tag{17}$$

Based on Equations (4) and (12) the stress increment will then result in:

$$d\underline{\sigma} = \underline{C}_e \cdot \left(d\underline{\varepsilon} - d\underline{\varepsilon}_p\right) = \underline{C}_e \cdot \left(d\underline{\varepsilon} - d\lambda \cdot \frac{\partial F}{\partial \underline{\sigma}}\right) \tag{18}$$

$$\Rightarrow d\underline{\sigma} = \left(\underline{C}_e - \frac{\underline{C}_e \cdot \partial F/\partial \underline{\sigma} \cdot \left[\underline{C}_e \cdot \partial F/\partial \underline{\sigma}\right]^T}{\left[\partial F/\partial \underline{\sigma}\right]^T \cdot \underline{C}_e \cdot \partial F/\partial \underline{\sigma} + 4 \cdot H \cdot \sigma_V^2}\right) \cdot d\underline{\varepsilon} = \left(\underline{C}_e - \underline{C}_p\right) \cdot d\underline{\varepsilon} \tag{19}$$

The equations derived are valid for arbitrary spatial stress states. In the following section they are explicitly expressed for practical applications on stress states of beam theory.

2.5 Explicit formulations for stress field of beam theory

As mentioned previously and exemplified in Figure 6, stresses σ_x, τ_{xy}, and τ_{xz} as well as corresponding strains are of vital importance in beam theory (i.e. $\sigma_y = \sigma_z = \tau_{yz} = 0$) and therefore combined in vectors:

$$\underline{\sigma}^T = [\sigma_x \quad \tau_{xy} \quad \tau_{xz}] \tag{20}$$

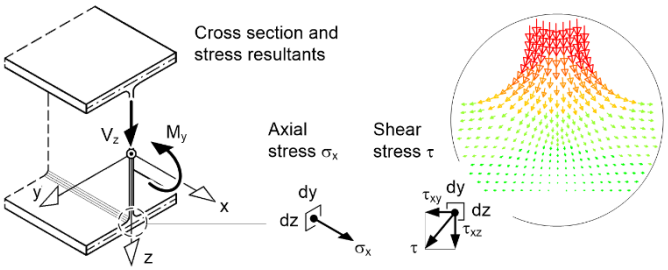

Figure 6 Stresses of beam theory for the example of uniaxial bending with shear

$$\underline{\varepsilon}^T = [\varepsilon_x \quad \gamma_{xy} \quad \gamma_{xz}] \tag{21}$$

This accounts for neglecting transverse contraction (Poisson's ratio) ν with regard to normal stress going along with the following elasticity matrix $\underline{C}_e$ as proper approximation:

$$\underline{C}_e = \begin{bmatrix} E & 0 & 0 \\ 0 & G & 0 \\ 0 & 0 & G \end{bmatrix} \tag{22}$$

The shear modulus is connected to the modulus of elasticity by $G = E/[2 \cdot (1 + \nu)]$. Considering the abovementioned stresses, the equivalent stress (9) and yield condition (10) are:

$$F = \sigma_V^2 - \kappa^2(\varepsilon_{p,V}) = 0 \tag{23}$$

$$\kappa = f_y + H \cdot \varepsilon_{p,V} \tag{24}$$

$$\sigma_V = \sqrt{\sigma_x^2 + 3(\tau_{xy}^2 + \tau_{xz}^2)} \tag{25}$$

With the derivatives of the yield condition in Equation (12)

$$\left[\frac{\partial F}{\partial \underline{\sigma}}\right]^T = [2 \cdot \sigma_x \quad 6 \cdot \tau_{xy} \quad 6 \cdot \tau_{xz}] \tag{26}$$

and the elasticity matrix (22) the proportionality factor $d\lambda$ according to Equation (17) becomes:

$$d\lambda = \frac{1}{2} \cdot \frac{E \cdot \sigma_x \cdot d\varepsilon_x + 3 \cdot G \cdot (\tau_{xy} \cdot d\gamma_{xy} + \tau_{xz} \cdot d\gamma_{xz})}{E \cdot \sigma_x^2 + 9 \cdot G \cdot (\tau_{xy}^2 + \tau_{xz}^2) + H \cdot \sigma_V^2} \tag{27}$$

Using Equations (18) or (19), respectively, gives the plastic constitutive matrix $\underline{C}_p$:

$$\underline{C}_p = \frac{1}{E \cdot \sigma_x^2 + 9 \cdot G \cdot (\tau_{xy}^2 + \tau_{xz}^2) + H \sigma_V^2} \cdot \begin{bmatrix} E^2 \cdot \sigma_x^2 & 3 \cdot E \cdot G \cdot \sigma_x \cdot \tau_{xy} & 3 \cdot E \cdot G \cdot \sigma_x \cdot \tau_{xz} \\ & 9 \cdot G^2 \cdot \tau_{xy}^2 & 9 \cdot G^2 \cdot \tau_{xy} \cdot \tau_{xz} \\ sym. & & 9 \cdot G^2 \cdot \tau_{xz}^2 \end{bmatrix} \tag{28}$$

With this and Equation (22) the correspondence between stress and strain increment

$$d\underline{\sigma} = (\underline{C}_e - \underline{C}_p) \cdot d\underline{\varepsilon} \tag{29}$$

is formulated. As can be seen, $\underline{C}_p$ leads to a reduction of stiffness when material plasticizes. In principle the derived equation corresponds to formulations specified in [8] or [12] for example. Since the constitutive Equation (28) depends on the stress state, a direct application of Equation (29) is difficult. However, it can be implemented productively using incremental procedures as shown in the next chapter. In order to make use of the yield condition (23), the equivalent strain $\varepsilon_{p,V}$ going along with a certain stress state is also needed. The increment of $\varepsilon_{p,V}$ connected to the incremental change of strains may be determined by introducing the proportionality factor $d\lambda$ (27) into Equation (15):

$$d\varepsilon_{p,V} = \frac{E \cdot \sigma_x \cdot d\varepsilon_x + 3 \cdot G \cdot (\tau_{xy} \cdot d\gamma_{xy} + \tau_{xz} \cdot d\gamma_{xz})}{E \cdot \sigma_x^2 + 9 \cdot G \cdot (\tau_{xy}^2 + \tau_{xz}^2) + H \cdot \sigma_V^2} \cdot \sigma_V \tag{30}$$

3 Application on thin walled cross-sections

3.1 Cross-section idealisation

In steel construction, cross-sections can in general by approximation be assumed to be compounded of several thin walled rectangular plates for reasons of simplicity. In doing so, the partial plates are reduced to their reference line, i.e. the thickness of each plate is scaled down to its middle line as shown in Figure 7. It is assumed that each individual plate is able to incorporate or resist, respectively, normal stress as well as shear stress along its middle line. Regarding this shear stress, a local coordinate s is introduced for the individual plates (see Figure 7). The shear stress is then connected to corresponding strains along the middle line. With respect to the previous chapter, shear stresses τ_{xy} and τ_{xz} are now described by τ_{xs} going along with the following stress-strain relationships:

$$\sigma_x = E \cdot \varepsilon_x \tag{31}$$

$$\tau_{xs} = G \cdot \gamma_{xs} \tag{32}$$

It is noteworthy mentioning, that shear stresses perpendicular to middle lines do not develop using this simplification. In addition, stresses σ_x and τ_{xs} are assumed to be constant within the plate thickness t. Shear stress distributions linear over t, as they arise in partial thin-walled rectangular plates for primary torsional loading, may therefore not directly be captured with this simplification.

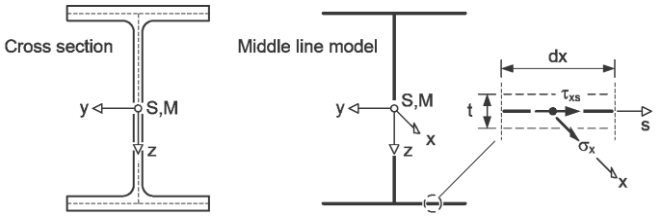

Figure 7 Cross-section, middle line model and corresponding stresses

When the section is divided by thin-plates, cross-section properties, stresses, and strains can be calculated using the middle line model (see [9] and [13]). As long as a cross-section is totally elastic, corresponding calculations may be performed using a rather coarse discretization for obtaining accurate results, e.g. as shown in Figure 8a. Regarding bending and shear force, the elastic stresses at any position of the cross-section are:

$$\sigma_x = -\frac{M_z}{I_z} \cdot y + \frac{M_y}{I_y} \cdot z \tag{33}$$

$$\tau_{xs} = -\frac{V_z \cdot S_y}{I_y \cdot t(s)} - \frac{V_y \cdot S_z}{I_z \cdot t(s)} \tag{34}$$

In these equations M_y and M_z are bending moments, V_y and V_z shear

forces, I_y and I_z moments of inertia, and S_y and S_z static moments. All values refer to the principal axes y and z of the cross-section.

However, for obtaining stresses and strains when plasticising, a finer discretization of the cross-section is needed, as can be seen in Figure 8b. In each fibre, the stress and strain evolution is followed in its midpoint as described in the next section and the values are assumed to be constant within the fibre. It is in the nature of things that an improvement of the mesh in terms of refinement will lead to higher accuracy in calculation results. For that reason, Figure 8b is only supposed to illustrate the discretization and plates have to be subdivided into many more elements for meaningful results, i.e. about 50 to 100 Elements for each plate.

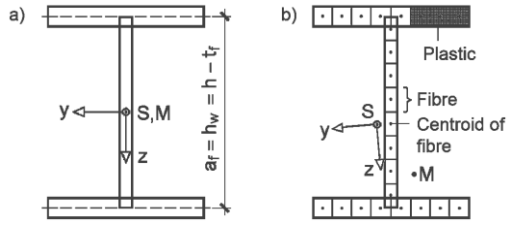

Figure 8 Cross-section discretization according to [7], a) Cross-section in the elastic range, b) fine discretization for states of plasticisation

3.2 Implementation of plasticity algorithm

To follow the stress and strain development, respectively, an incremental and iterative procedure is set up when fibres of the cross-section start to plasticise. For that purpose, so called predictor-corrector algorithms are in general used. For instance [9] gives first impression, how formulations based on an elastic predictor and the use of the proportionality factor $d\lambda$ for the corrector can be applied. Here, an approach based on [14] is used for the corrector.

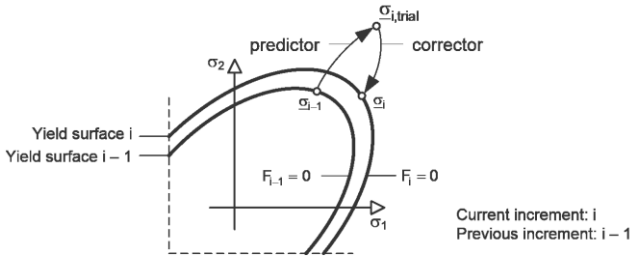

Figure 9 Predictor stress state and corrector stress vector according to [9]

For the incremental approach, a strain increment needs to be defined. For that purpose, elastic stresses and strains are determined in each fibre of the cross-section on the basis of Equations (33) and (34). Based on Equation (21), the strain increment in a certain fibre is assumed to be part of the previously determined elastic strains:

$$\Delta\underline{\varepsilon}^T = [\Delta\varepsilon_x \quad \Delta\gamma_{xy} \quad \Delta\gamma_{xz}] \tag{35}$$

In each fibre of the cross-section, the strain increments are applied stepwise and for each strain increment an iteration is conducted if necessary. Regarding a current incremental strain step of a certain fibre indicated by the index i, it assumed that the stress and strain states $\underline{\sigma}_{i-1}$ and $\underline{\varepsilon}_{i-1}$ as well as the plastic constitutive matrix $\underline{C}_p = \underline{C}_p(\underline{\sigma}_{i-1})$ according to Equation (28) and the equivalent plastic strain $\varepsilon_{p,V} = \varepsilon_{p,V,i-1}$ (cumulated strains of Equation (30)) of a previous step $i-1$ are known. Using Equation (29), the application of the strain increment leads to following expressions:

$$\underline{\varepsilon}_i = \underline{\varepsilon}_{i-1} + \Delta\underline{\varepsilon} \tag{36}$$

$$\Delta\underline{\sigma} = \left(\underline{C}_e - \underline{C}_p\right) \cdot \Delta\underline{\varepsilon} \tag{37}$$

$$\underline{\sigma}_{i,trial} = \underline{\sigma}_{i-1} + \Delta\underline{\sigma} \tag{38}$$

This stress state is designated as predictor. The additional stresses $\Delta\underline{\sigma}$ are determined using the constitutive elasto-plastic relationship of the previous step. This can in general only be a certain approximation, since the constitutive relationship will also be influenced by $\Delta\underline{\sigma}$. The increment of the equivalent plastic strain $\Delta\underline{\varepsilon}_{p,V}$ due to the strain increment $\Delta\underline{\varepsilon}$ is given by Equation (30). Introducing the stress state of $\underline{\sigma}_{i,trial}$ leads to:

$$\underline{\varepsilon}_{p,V,i} = \underline{\varepsilon}_{p,V,i-1} + \Delta\underline{\varepsilon}_{p,V}\left(\Delta\underline{\varepsilon}, \underline{\sigma}_{i,trial}, \sigma_V\left(\underline{\sigma}_{i,trial}\right)\right) \tag{39}$$

As long as the fibre is within the elastic range, i.e. $\varepsilon_{p,V,i} = 0 \Longrightarrow \kappa\left(\varepsilon_{p,V,i}\right) = f_y$, the yield condition (23) with

$$F = \sigma_V^2\left(\underline{\sigma}_{i,trial}\right) - \kappa^2\left(\varepsilon_{p,V,i}\right) \leq 0 \tag{40}$$

will be satisfied and the trial stress field of the predictor reflects the stress state of the regarded increment, i.e. $\underline{\sigma}_i = \underline{\sigma}_{i,trial}$.

In case $F > 0$ according to Equation (39) (stress is outside yield surface), the trial stress state is not possible and therefore invalid. Using a so-called corrector stress vector, the predictor is returned to a valid state in which it is $F = 0$ (Figure 9). The corrector is defined as a vector following the opposite direction of the stress evolution back to the yield surface. The orientation of this vector is assumed to be normal to the yield surface and can therefore be described by the derivatives of the yield condition as shown in [14] giving

$$\Delta\underline{\sigma} = \partial F / \partial\underline{\sigma} \cdot p, \tag{41}$$

where p is a scalar value to be determined. The correcting stresses lead to a variation of equivalent stress $\Delta\sigma_V$. Considering this variation, the yield condition (40) is to be satisfied, i.e. $F = 0$. Introducing the differential for $\Delta\sigma_V$ and Equation (41) gives an expression for p:

$$F = (\Delta\sigma - \Delta\sigma_V)^2 - \kappa^2 = \left(\Delta\sigma - \left[\partial\sigma_V/\partial\underline{\sigma}\right]^T \cdot \Delta\underline{\sigma}\right)^2 - \kappa^2 = 0 \tag{42}$$

$$\Longrightarrow \Delta\sigma - \kappa = \left[\partial\sigma_V/\partial\underline{\sigma}\right]^T \cdot \partial F/\partial\underline{\sigma} \cdot p \Longrightarrow p = \frac{\Delta\sigma - \kappa}{\left[\partial\sigma_V/\partial\underline{\sigma}\right]^T \cdot \partial F/\partial\underline{\sigma}}$$

With this, the corrector stresses of Equation (41) are:

$$\Delta\underline{\sigma} = \frac{\Delta\sigma - \kappa}{\left[\partial\sigma_V/\partial\underline{\sigma}\right]^T \cdot \partial F/\partial\underline{\sigma}} \cdot \partial F/\partial\underline{\sigma} \tag{43}$$

The derivatives of the yield condition $\partial F/\partial\underline{\sigma}$ for a stress state of beam theory are specified in Equation (26). Supplementing the derivatives of the $\partial\sigma_V/\partial\underline{\sigma}$ of the equivalent stress with

$$\left[\frac{\partial\sigma_V}{\partial\underline{\sigma}}\right]^T = \frac{1}{\sigma_V} \cdot [\sigma_x \quad 3\cdot\tau_{xy} \quad 3\cdot\tau_{xz}] \tag{44}$$

and considering the trial stress vector $\underline{\sigma}_{i,trial}$ as well as the equivalent plastic strain $\varepsilon_{p,V,i}$ (in κ according to the yield condition in Equation (40)) leads to the following corrector:

$$\Delta\underline{\sigma} = \frac{\left[\sigma_V\left(\underline{\sigma}_{i,trial}\right) - \kappa\left(\varepsilon_{p,V,i}\right)\right] \cdot \sigma_V\left(\underline{\sigma}_{i,trial}\right)}{\sigma_{x,i,trial}^2 + 9\cdot\left(\tau_{xy,i,trial}^2 + \tau_{xz,i,trial}^2\right)} \cdot \begin{bmatrix} \sigma_{x,i,trial} \\ 3\cdot\tau_{xy,i,trial} \\ 3\cdot\tau_{xz,i,trial} \end{bmatrix} \tag{45}$$

Stresses going along with the applied strain increment can now be described by the following formula

$$\underline{\sigma}_{i,corr} = \underline{\sigma}_{i,trial} - \Delta\underline{\sigma}, \tag{46}$$

in which the subscript "*corr*" accounts for corrected. If the yield condition

$$F = \sigma_V^2\left(\underline{\sigma}_{i,corr}\right) - \kappa^2\left(\varepsilon_{p,V,i}\right) = 0 \tag{47}$$

is not fulfilled sufficiently exact, another iteration for correcting stresses may be executed, in which the new trial stress is assumed to be the corrected stress calculated, i.e. $\underline{\sigma}_{i,trial} = \underline{\sigma}_{i,corr}$. Otherwise, the stress state of increment i is determined with $\underline{\sigma}_i = \underline{\sigma}_{i,corr}$ and the next strain increment may be applied by adjusting the constitutive matrix by $\underline{C}_p = \underline{C}_p\left(\underline{\sigma}_i\right)$ and restarting the algorithm using equation (36). It is noteworthy mentioning, that when starting the incremental algorithm and accounting for the very first strain increment, the stress vector and the strain vector are assumed to be zero, i. e. $\underline{\sigma} = \underline{\varepsilon} = \underline{0}$. The cross-section is therefore assumed to be totally elastic and the plastic part of the elasto-plastic constitutive matrix of Equation (29) is a zero matrix as well, i.e. $\underline{C}_p = \underline{0}$. The whole algorithm is visualized in Figure 10.

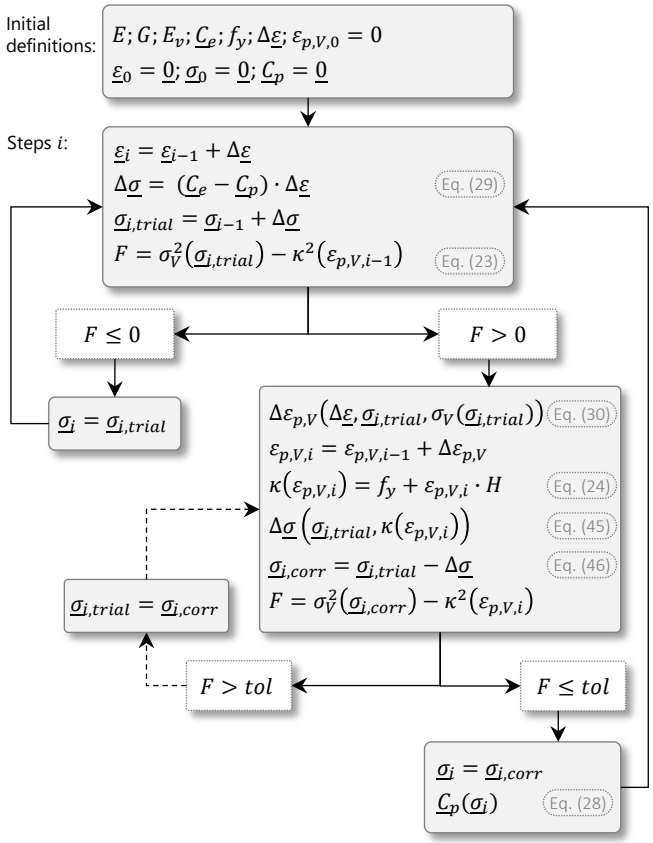

Figure 10 Plasticity algorithm for 2D stress states

4 Calculation examples

4.1 Comparison to software

The algorithm described in the previous chapter has been implemented in an intern software. In this section it is validated by comparing results with a sophisticated FE numerical software (ANSYS). For that purpose, a numerical model of a beam is generated with the commercial software and the plasticisation of the beam is observed for defined load situations. The numerical model uses shell elements, i.e. 5 degrees of freedom per node considering two axial stresses and the corresponding shear stress. Extracting stress-strain developments of fibres from the beam model allows comparison to the stress-strain evolution resulting from the algorithm of section 3.2.

The parameters of the material law considered in the analyses are described in Table (1). The tangent modulus E_v is chosen to be comparably large for calculations considering a yield plateau, however, is within a typical range when strain hardening effects are to be accounted.

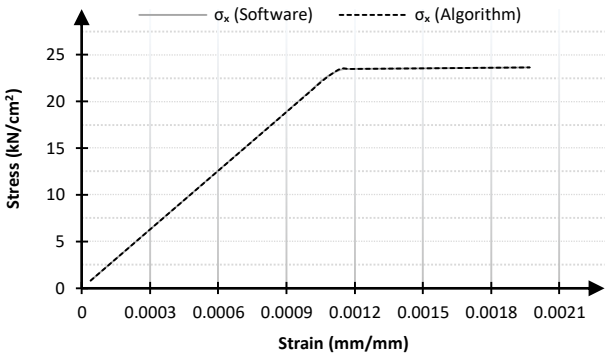

Figure 11 Axial stresses comparison

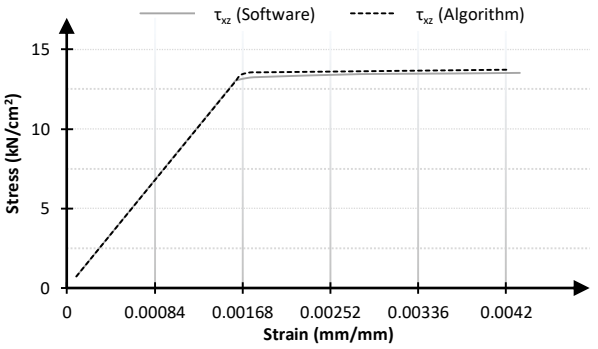

Figure 12 Shear stresses comparison

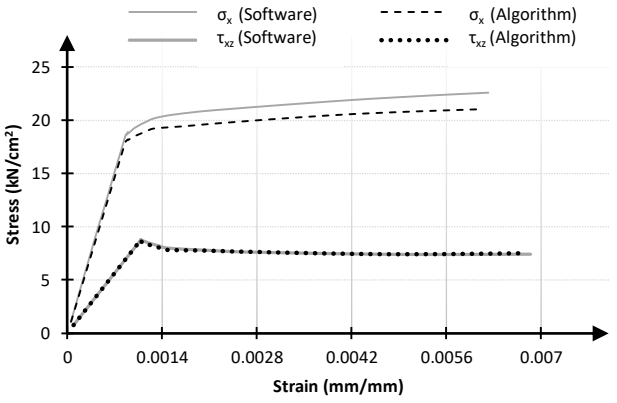

Figure 13 Combined stresses comparison (axial and shear stresses)

Figures 11 to 13 show the stress paths of the extracted fibre from the commercial software in comparison to the results of the plasticity algorithm. In Figure 11, a fibre connected to normal stress is regarded ($\tau = 0$). The plot illustrates that the axial stresses calculated by the algorithm follow the axial stresses from the software perfectly. In case of pure shear stresses ($\sigma_x = 0$), the results show good agreement as well, as can be seen in Figure 12. Here, small deviations of 2% magnitude are noticeable due to the existence of further stress components in the shell model comparable to the explanations below.

Figure 13 shows comparisons of a combined stress state considering normal and shear stresses. The shear stresses calculated using the algorithm match the results of the software in the elastic and plastic state very good. However, for axial stresses, the results indeed show good agreement in the elastic range, while in the plastic state considerable deviations are visible. These deviations are a result of normal stresses in *z* direction appearing in the commercial software due to the use of shell elements. With regard to beam theory, they are neglected in the algorithm of section 3.2. Figure 14 shows the stress values of σ_z which increase up to 3 kN/cm² in the plastic state. With Equation (9) it can be noticed that σ_z directly interacts with σ_x, leading to the differences in Figure 13.

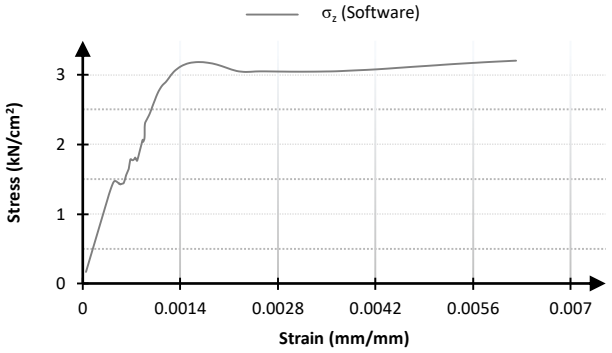

Figure 14 Stresses in z direction (commercial software)

Table 1 Material properties

Elasticity (E) :	21 000 (kN/cm²)
Tangent modulus (E_v) :	210 (kN/cm²)
Shear Modulus (G) :	8070 (kN/cm²)
Yielding capacity (f_y) :	23.5 (kN/cm²)

4.2 Implementation of plasticity in the cross-section

4.2.1 Preliminary remarks

In this section, the plasticity algorithm is combined with the cross-sectional analysis. In the following, different cases are presented considering bending or shear stresses only in section 4.2.2 and combined stress states in 4.2.3. The cross-section evaluated corresponds to an IPE120 ($h = 120\ mm$; $b = 64\ mm$; $t_w = 4.4\ mm$; and $t_f = 6.3\ mm$) using the cross-section modelling shown in Figures 7 and 8. The material properties are compiled in Table 1, except for the tangent modulus E_v, which is assumed to be 2.1 kN/cm².

The procedure for evaluating the plasticization of the cross-section is described in chapter 3. First, forces and moments are applied to the section and the stresses in each fibre are evaluated along with the corresponding strains according to theory of elasticity. Then, incremental strains are defined as a fraction of these elastic strains. For each incremental strain step, the stresses are determined according to the plastic algorithm described in section 3.2. For evaluating internal forces corresponding to stress states, the stresses are integrated over the cross-section.

4.2.2 Individual acting of bending or shear stresses

When performing the incremental strain analysis with regard to bending stress, the elastic limit is reached for $M_y = 1301\ kNcm$. The value shows good agreement with a manual calculation of the elastic bending capacity. In the case of plastic limit, the incremental cross-section analysis results in $M_y = 1434\ kNcm$, showing also good correlation to analytical calculations and literature [13]. In Figure 15, the stress distributions in the elastic and plastic states are shown.

When applying the algorithm for shear stresses, the shear capacity of the section in the elastic range is $V_z = 62.5\ kN$, while in the plastic it is $V_z = 69.0\ kN$. Both values agree with manual calculation of elastic and plastic capacities. The stresses are shown in Figure 16.

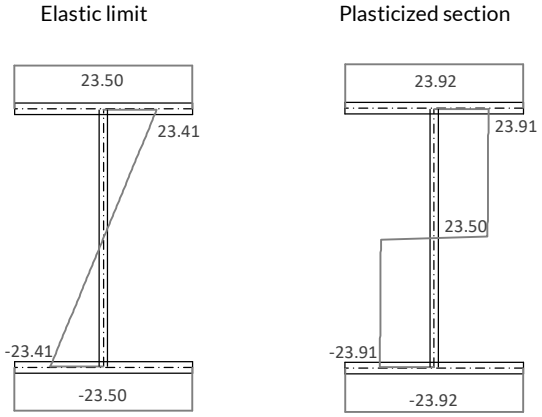

Figure 15 Axial stresses [kN/cm²] in cross-section for bending moment force

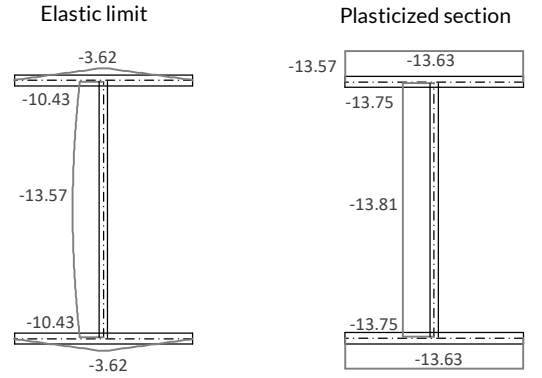

Figure 16 Shear stresses [kN/cm²] in cross-section for shear force

4.2.3 Combined stress states

Regarding combined stress states of shear and normal stresses, first a low shear force combined with a high bending moment is applied. The stresses in the plastic state are shown in Figure 18. As can be seen, axial stresses in the web are not linear due to shear stress components. Shear stresses tend to concentrate close to the centroid, being responsible for plasticity in that region. In this case, the bending moment and the shear force corresponding to the stress states of Figure 18 are $M_y = 1410\ kNcm$ and $V_z = 31.6\ kN$.

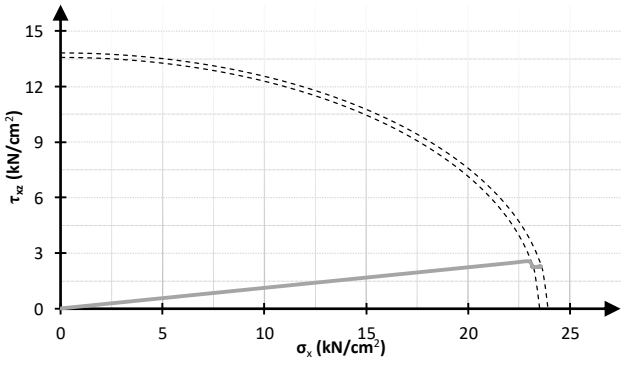

Figure 17 Stress development in the 2D stress space surface

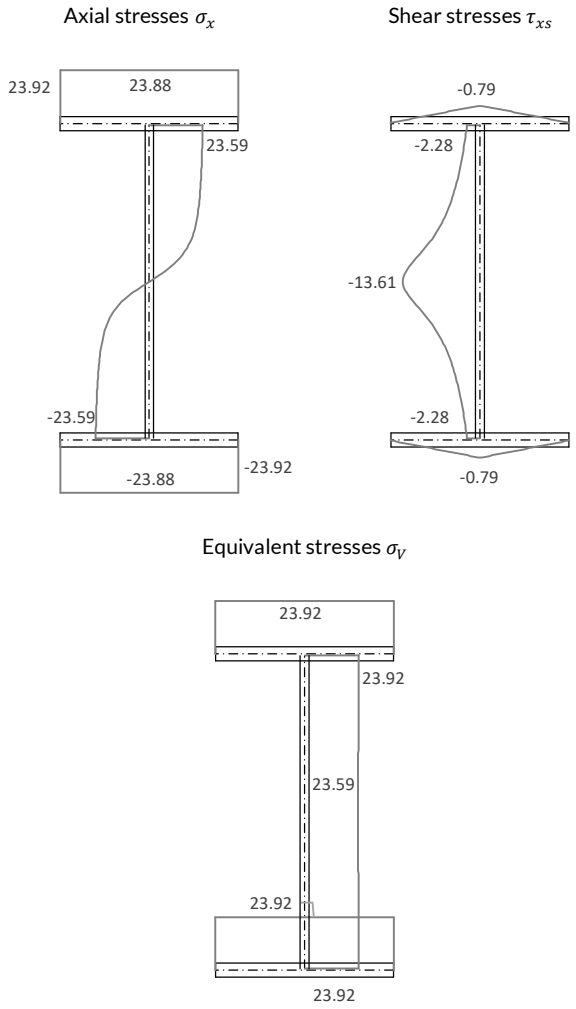

Figure 18 Axial, shear, and equivalent stresses [kN/cm^2] for combined states with comparably higher bending and lower shear

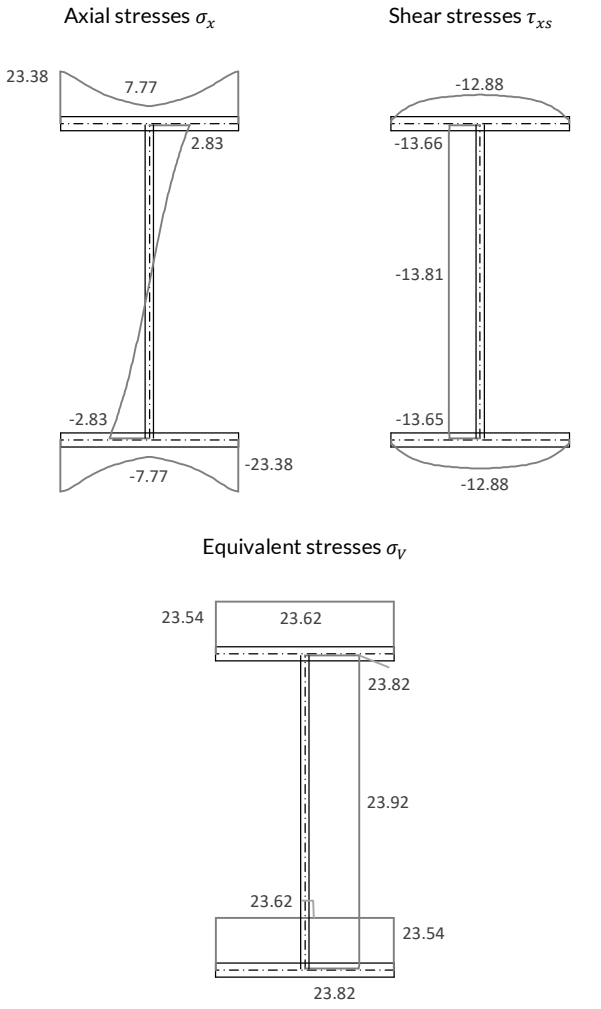

Figure 19 Axial, shear, and equivalent stresses [kN/cm^2] for combined states with comparably lower bending and higher shear

The stress development at the bottom edge of the web is shown in the two-dimensional stress space in Figure 17 (for plotting purposes, stresses are considered as positive). In Figure 17, the yield surface of the elastic limit ($\sigma_V = 23.5\ kN/cm^2$) as well as the one for an equivalent strain of 0.2 mm/mm ($\sigma_V = 23.92\ kN/cm^2$) are shown. As can be seen, when strains are incremented gradually, shear stress reduces after reaching the first yield surface. This exemplifies the redistribution of stress with the beginning of plasticising.

The second evaluation of combined stresses is performed using a higher shear force and correspondingly lower bending moment. The results of the stress distribution are displayed in Figure 19, showing differences compared to the previous example. Here, axial stresses are reduced in the web of the profile while shear stresses show a more uniform distribution along the web. Regarding the flanges, axial stresses are higher in the edges and reducing to the centre. In this example, the bending moment corresponding to Figure 19 is $M_y = 678\ kNcm$ and the shear force is $V_z = 68.3\ kN$.

5 Summary, conclusions and outlook

In this paper, the derivation and implementation of plastic cross-sectional analysis is presented. Explicit formulations for stress states of beam theory are introduced and implemented by an incremental algorithm for evaluating plasticization of a material fibre. Comparisons of algorithm results with sophisticated FE software are presented for reasons of validation leading to good correlations.

Afterwards, the algorithm is implemented in cross-section analyses using the middle line method. It is shown that plasticity of combined stress states regarding normal and shear stresses is encountered properly using the approach. Moreover, the stress evolution of fibres as well as the interaction between shear and bending can be studied.

Future work will focus on merging cross-section analyses with finite beam elements for obtaining a global analysis of structures under plastic considerations. Moreover, the consideration of residual stresses in the cross-section is to be addressed as well.

References

[1] Simo, J.C.; Hughes, T.J.R. (1998) Computational inelasticity. New York: Springer-Verlag.

[2] Lemaitre, J.; Chaboche, J.L. (1990) *Mechanics of solid materials*. New York: Cambridge University Press.

[3] Chen, W.F.; Han, D.J. (1988) *Plasticity for structural engineers*. New York: Springer-Verlag.

[4] Wu, H.C. (2005) *Continuum mechanics and plasticity*. New York: Chapman & Hall/CRC.

[5] Krabbenhoft, K (2002) *Basic computational plasticity*. Department of civil engineering: Technical university of Denmark.

[6] Öchsner, A. (2014) *Elasto-Plasticity of frame structures elements:*

modeling and simulation of rods and beams. Berlin: Springer-Verlag.

[7] Kindmann, R.; Kraus, M. (2019) *FE-Berechnungen mit Fließzonen für Tragfähigkeitsnachweise nach DIN EN 1993-1-1*. Berlin: Ernst & Sohn.

[8] Chen, G.; Trahair, N.S. (1992) *Inelastic nonuniform torsion of steel I-beams*. J. Constructional steel research 23(1-3), p. 189-207.

[9] Kraus, M.; Kindmann, R. (2019) *Finite-Elemente-Methoden im Stahlbau*. 2. Aufl. Berlin: Verlag Ernst & Sohn.

[10] DIN EN 1993-1-1: 12-2010, Eurocode 3 – Bemessung und Konstruktion von Stahlbauten; Allgemeine Bemessungsregeln unf Regeln für den Hochbau.

[11] Gross, D.; Seelig, T. (2016) *Bruchmechanik*. Berlin Heidelberg: Verlag Springer Vieweg.

[12] Sapountzakis, E. J. (2013) *Bars under Torsional Loading: A Generalized Beam Theory Approach*. ISRN Civil Engineering 2013, Article ID916581.

[13] Kindmann, R.; Kraus, M.; Niebuhr, H. J. (2017) *STAHLBAU KOMPAKT, Bemessungshilfen, Profiltabellen*. 4. Aufl. Düsseldorf: Verlag Stahleisen.

[14] Nayak, G.C.; Zienkiewicz, O.C. (1972) *Elasto-plastic stress analysis – A Generalization for various constitutive realisations including strain softening*. J. for numerical methods in engineering 5(1), p. 113-135.